Peer-reviewed version available at *Appl. Sci.* **2020**, *10*, 5067; doi:10.3390/app10155067

Article

Truck platoon control considering heterogeneous vehicles

Jonghoek Kim [1,*]

[1] Electrical and Electronic Convergence Department, Hongik University, Sejong-city, South Korea
* Correspondence: jonghoek@hongik.ac.kr

Abstract: This paper presents control algorithms enabling autonomous heterogeneous trucks to drive in platoons. Heterogeneous trucks imply that the hardware information (e.g., truck length, break, accelerator, or engine) of a truck may be distinct from that of another truck. We define a platoon as a collection of trucks where a manually driven truck (leader truck) is followed by several automatically controlled following trucks. The proposed approach is to make every autonomous truck keep following the leader's trajectory while maintaining a designated distance from its predecessor truck. As far as we know, this paper is unique in developing both lateral maneuver and speed control considering a platoon of heterogeneous trucks. The efficiency of the proposed approach is verified using simulations.

Keywords: platoon of heterogeneous trucks; lateral maneuvers; longitudinal maneuvers; truck platoon; multi-agent systems; autonomous trucks;

1. Introduction

This paper is on developing technology that enables autonomous heterogeneous trucks to drive in platoons. We define a platoon as a collection of trucks where a manually driven truck (leader truck) is followed by several automatically controlled following trucks. It is well known that a truck platooning can reduce fuel consumption of a following truck considerably [1–3].

In the literature on autonomous cars, many works have been done on tracking a curve (lane for autonomous cars) while avoiding collision assisted by various sensors [4–9]. Specifically, [4] proposed a lane detection algorithm based on Support Vector Machines (SVM) classifier, and splines based lane model combined with Kalman filters was used for the tracking algorithm. [5] presented a method of detecting and tracking the boundaries of drivable regions in a road without road-markings. Using vision sensors, an autonomous truck can follow a lane. However, vision sensors may not work in the case where a lane is not clearly visible. Moreover, there may be a case where a vision sensor on an autonomous car is disabled.

This paper considers the scenario where the leader truck is driven by a trained truck driver. A trained driver has the ability to perform reliable driving in unstructured environments. For instance, a human driver can control a truck even in environments where there is no lane. Thus, this paper considers the scenario where the leader truck is driven by a trained truck driver. Then, all autonomous trucks follow the leader's trajectory.

In summary, driving in truck platoons has the following benefits: 1. fuel consumption decreases compared to the case where the trucks do not form a platoon. 2. the trained truck driver can lead the platoon even in unstructured environments.

There are many papers on control of truck platoon [1–3,10–15]. [16] showed that limiting truck platoons on the special lane can higher the average speed of traffic flow and reduce the lane changing frequency.

An autonomous truck must change its speed to maintain a designated distance with its predecessor truck. Controlling the speed of a truck is called the *longitudinal control* of the truck. Many papers handled longitudinal control of truck platoon [1,11–15,17,18]. Longitudinal control was developed based on a distributed controller known as Cooperative Adaptive Cruise Control (CACC) [19]. [20] considered both communication and parasitic delays in the design of longitudinal control of truck platoon. Considering longitudinal control, the authors of [10,21] analyzed the string stability of platoons of Adaptive Cruise Control (ACC) trucks. [22] used consensus control strategy for longitudinal control of truck platoons. The consensus control is used to make the speed of every vehicle converge to the speed of the leader.

In [23], the problem of longitudinal control of networked intelligent vehicles with external disturbance and network-induced disturbance was studied. [24] present a two-layered hierarchical framework for truck platoon speed control: a speed planning layer for en route speed profile calculation and a control layer for vehicle speed tracking. [25] handled the adaptive longitudinal control of 1-D platoon of non-identical (heterogeneous) vehicles.

In practice, truck platoon must perform lateral maneuver as well as speed control. Suppose that the leader finds an obstacle ahead of it. In this case, the leader avoids the obstacle by changing its lane. Then, the following autonomous trucks need to change their lanes to avoid the obstacle. This implies that both lateral maneuver and speed control are crucial for truck platoon control. Thus, this paper integrate both lateral maneuver and speed control of truck platoon.

In this paper, the following trucks follow waypoints along the trajectory of the leader. The yaw of an autonomous truck is controlled to make it visit the leader's waypoints sequentially. As the leader changes its lane to avoid collision with an obstacle in front of it, every following truck changes its lane by following waypoints of the leader. Also, we control the speed of each truck so that every autonomous truck keeps following the waypoints while maintaining a designated distance from its predecessor truck.

As far as we know, this paper is unique in handling both lateral maneuver and speed control considering heterogeneous trucks. Heterogeneous trucks imply that the hardware information (e.g., truck length, break, accelerator, or engine) of a truck may be distinct from that of another truck. This is a feasible scenario, since the functionality of a truck's hardware system (e.g., break, accelerator, or engine) gets worse as time goes on. Thus, we argue that no two trucks are identical in practice. Also, there may be a practical scenario where we need to use various trucks with distinct size.

This paper presents both lateral maneuver and speed control considering heterogeneous trucks. The efficiency of the proposed approach is verified using simulations.

This paper is organized as follows. Section 2 presents definitions and assumptions used in the paper. Section 3 presents the multi-vehicle control proposed in this paper. Section 4 presents MATLAB simulations to verify the effectiveness of our control laws. Section 5 provides Conclusions.

2. Definitions and Assumptions

Suppose that there are N heterogeneous trucks. p^i denotes the i-th truck ($i \in \{1, 2, ..., N\}$). The predecessor of p^{i+1} is p^i. p^1 is the leader truck driven by a trained truck driver.

We consider discrete-time systems. Let T denote the sampling interval. The subscript k denotes the time step k. $\mathbf{P}^i_k$ denotes the position of the i-th truck at time step k.

We consider the global coordinate system to present the motion model of a truck. The global coordinate of a truck p^i is given by $\mathbf{P}^i_k = [x^i_k, y^i_k]^T$, while its orientation in the global frame is represented by ψ^i_k. In the body frame of p^i, δ^i_k is the steering angle of the truck at time step k.

The truck's speed at time step k is s^i_k in the truck's x-direction (body frame), and zero in the y-direction (body frame), since this paper assumes that the wheels cannot slip sideways [1].

Peer-reviewed version available at Appl. Sci. 2020, 10, 5067; doi:10.3390/app10155067

If the front wheel is located at distance L^i from the rear wheel along the orientation of the truck p^i, then the Ackermann Steering model[26] is

$$\begin{aligned} x^i_{k+1} &= x^i_k + T * s^i_k * \sin(\psi^i_k), \\ y^i_{k+1} &= y^i_k + T * s^i_k * \cos(\psi^i_k), \\ \psi^i_{k+1} &= \psi^i_k + T * \frac{s^i_k}{L^i} \tan(\delta^i_k). \end{aligned} \tag{1}$$

In Ackermann steering model, each wheel has its own pivot point and the system is constrained in such a way that all wheels of the car drive on circles with a common center point, avoiding skid [26]. We acknowledge that in the case where slip sideways are allowed, more complicated truck models in [27–29] are required. However, as we consider slip sideways, we need to set various parameters, such as the truck mass or inertia.

Considering heterogeneous trucks, each truck has distinct motion model from other trucks. Setting complicated models for each individual truck is time-consuming, and a truck's model may not represent the true dynamics of the truck as the truck runs a longer distance. For instance, the functionality of a truck's hardware (such as engine, accelerator, or braking system) gets worse as time goes on. Also, various road (or tire) situations may make effects on slip sideways. Accurate motion modeling in various environments may be impossible in practice.

(1) can handle heterogeneous trucks by allowing $L^i \neq L^j$ for $j \neq i$. $L^i \neq L^j$ implies that the length of the i-th truck is distinct from that of the j-th truck. Thus, this paper uses (1) as the motion model of each heterogeneous truck.

A car cannot arbitrarily change its speed within one time step. Thus, let a^i_A denote the maximum acceleration of a truck p^i. Also, let a^i_D denote the maximum deceleration of p^i. Here, a^i_A and a^i_D are determined by hardware information of p^i, such as engine, accelerator, or braking system of p^i. This implies that

$$s^i_{k-1} - a^i_D * T \leq s^i_k \leq s^i_{k-1} + a^i_A * T. \tag{2}$$

(2) presents the feasible range of s^i_k considering the maximum acceleration and deceleration of p^i. The maximum speed of p^i is s^i_M, i.e. $s^i_k \leq s^i_M$ for all k.

Considering heterogeneous trucks, $a^i_A \neq a^j_A$ ($\forall j \neq i$) is feasible. Also, $a^i_D \neq a^j_D$ ($\forall j \neq i$) is feasible. This is due to the fact that the hardware information (such as engine or braking system) of p^i may be distinct from that of p^j.

A car cannot change its heading abruptly between adjacent time steps, due to the car's geometry such as the maximum steering angle of the car. Let $\dot{\psi}^i_M$ present the maximum yaw rate of p^i. We have

$$\|\psi^i_{k+1} - \psi^i_k\| \leq \dot{\psi}^i_M T. \tag{3}$$

Let δ^i_M denote the maximum steering angle of a truck p^i. Then, $\dot{\psi}^i_M$ is derived as

$$\dot{\psi}^i_M = \frac{s^i_k}{L^i} \tan(\delta^i_M). \tag{4}$$

This implies that as the length of a truck p^i increases, the maximum yaw rate of p^i decreases. Also, as the maximum steering angle of p^i increases, the maximum yaw rate of p^i increases. Since we consider heterogeneous trucks, $L^i \neq L^j$ ($\forall j \neq i$) is feasible. Thus, $\dot{\psi}^i_M \neq \dot{\psi}^j_M$ ($\forall j \neq i$) is also feasible.

3. Multi-vehicle control

This paper considers the scenario where the leader truck is driven by a trained truck driver. Our approach is to make all trucks follow the leader's trajectory.

Whenever the leader travels Th meters, the leader's position is stored as *waypoint* for the following trucks. Let W_m denote the m-th waypoint. This implies that waypoints are generated as $W_1, W_2, ...,$ in this order. The distance between W_m and W_{m-1} is Th by its definition. Also, as a waypoint W_m is

Peer-reviewed version available at Appl. Sci. 2020, 10, 5067; doi:10.3390/app10155067

generated, we generate the curvature of the leader's path at the point. This curvature can be derived using the steering input of the leader at the point. Let K_m denote the curvature at W_m.

An autonomous truck keeps tracking the leader by following the waypoints of the leader. Whenever a following truck's distance from a waypoint W_{m-1} is less than Th, the truck heads towards the next waypoint W_m.

Using V2V communication [30], the leader's information (W_m and K_m) is transmitted to every following truck. At each time step k, the leader's information (W_m and K_m) is transmitted to every other truck in real time.

3.1. Longitudinal control

We describe how to control the speed of each truck for longitudinal control of the truck. The leader is controlled using ACC so that it maintains a constant speed. Also, the speed of a following autonomous truck is controlled to maintain a desired distance (reference platooning distance) from its predecessor truck.

The reference platooning distance at time step k for a truck p^i is denoted as d^i_k. This implies that the desired distance between p^i and p^{i-1} at time step k is d^i_k.

The main source of time delay between trucks is from the parasitic time delay induced by the mechanical systems and the communication delay generated by the communication and computing devices. We assume that the time delay in communication between the leader and a truck p^i is bounded by a certain constant, say t_d.

The travel distance of p^i within t_d seconds can be estimated as $t_d * s^i_k$. In order to avoid collision due to delayed communication, the reference distance d^i_k is set as a bigger value than $t_d * s^i_k$. Also, we set the lower bound for d^i_k for the safety of trucks. Let $min_D > 0$ present the lower bound for d^i_k. We use

$$d^i_k = g * t_d * s^i_k + min_D. \tag{5}$$

Here, $g \geq 1$ and min_D are positive constants. As the speed of a truck converges to s^1, d^i_k converges to $g * t_d * s^1 + min_D$, which is a positive constant. This separation change approach in (5) was inspired by the constant time headway spacing policy, which was also used in [21].

Suppose that p^i visited a waypoint W_{n-1} and is heading towards the next waypoint W_n. The curvature at W_{n-1} is K_{n-1}, and the curvature at W_n is K_n. Since p^i and p^{i-1} are adjacent trucks, assume that both p^i and p^{i-1} move along an arc path with radius, say $R = \frac{2}{K_n+K_{n-1}}$. See Figure 1. The arc path connecting p^i and p^{i-1} is depicted with a bold arc in this figure.

The distance between p^i and p^{i-1} at time step k is $D^{i-1,i}_k = \|\mathbf{P}^i_k - \mathbf{P}^{i-1}_k\|$. The arc angle associated to $D^{i-1,i}_k$ is

$$\theta = acos(\frac{2R^2-(D^{i-1,i}_k)^2}{2R^2}). \tag{6}$$

Recall that the desired distance between p^i and p^{i-1} at time step k is d^i_k. The arc angle associated to d^i_k is

$$\theta_d = \frac{d^i_k}{R}. \tag{7}$$

At time step k, p^{i-1} moves along the arc path with speed s^{i-1}_k within one sampling interval. The arc angle associated to the travel distance $s^{i-1}_k T$ is

$$\theta_s = \frac{s^{i-1}_k T}{R}. \tag{8}$$

Note that p^{i-1} is the predecessor of p^i, thus it moves away from p^i.

At each time step k, the i-th truck sets its reference speed, say r^i_k, as follows.

$$r^i_k = (\theta - \theta_d + \theta_s) * \frac{R}{T}. \tag{9}$$

Preprints (www.preprints.org) | NOT PEER-REVIEWED | Posted: 7 June 2020 doi:10.20944/preprints202006.0066.v1

Peer-reviewed version available at Appl. Sci. 2020, 10, 5067; doi:10.3390/app10155067

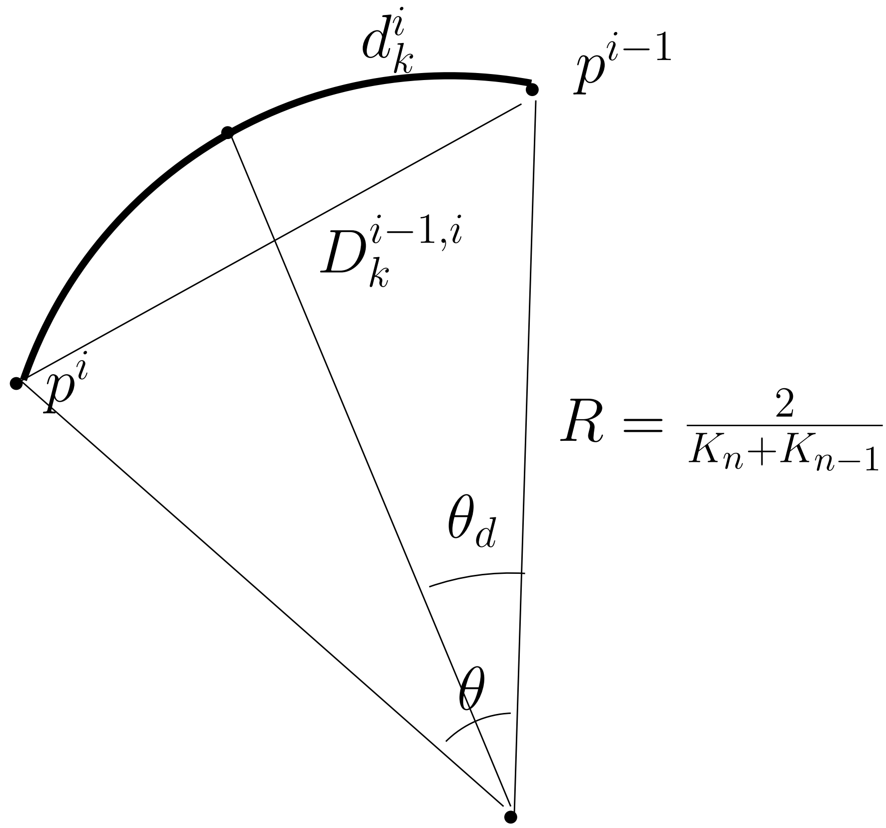

Figure 1. Since p^i and p^{i-1} are adjacent trucks, assume that both p^i and p^{i-1} are on an arc path with radius, say $R = \frac{2}{K_n+K_{n-1}}$. The arc path connecting p^i and p^{i-1} is depicted with a bold arc in this figure.

In the case where both p^i and p^{i-1} move along a straight path, R in (6) is ∞. (9) is not well-defined in this case. In the case where both p^i and p^{i-1} move along a straight path, the following equation is used to set the reference speed r_k^i.

$$r_k^i = \frac{D_k^{i-1,i} - d_k^i + s_k^{i-1}T}{T}. \tag{10}$$

Recall that the leader is controlled using ACC so that it maintains a constant speed. While the leader moves using ACC, we set the bound for r_k^i as

$$r_k^i \le \gamma * s_k^{i-1}. \tag{11}$$

This implies that if r_k^i using (9) or (10) is above $\gamma * s_k^{i-1}$, then we set

$$r_k^i = \gamma * s_k^{i-1}. \tag{12}$$

137 (12) implies that the reference speed of p^i cannot be much faster than the speed of p^{i-1}. The effect
138 of changing γ is analyzed in Section 4.

The reference speed r_k^i is used to change the speed of the truck at each time step. In the case where $r_k^i > s_{k-1}^i + a_A^i * T$, the reference speed r_k^i cannot be reached within one time step. Thus, we use

$$s_k^i = s_{k-1}^i + a_A^i * T. \tag{13}$$

Preprints (www.preprints.org) | NOT PEER-REVIEWED | Posted: 7 June 2020 doi:10.20944/preprints202006.0066.v1

Peer-reviewed version available at Appl. Sci. 2020, 10, 5067; doi:10.3390/app10155067

In the case where $r^i_k < s^i_{k-1} - a^i_D * T$, r^i_k cannot be reached within one time step. Thus, we use

$$s^i_k = s^i_{k-1} - a^i_D * T. \tag{14}$$

Otherwise, the reference speed r^i_k can be reached within one time step. Thus, we can set

$$s^i_k = r^i_k. \tag{15}$$

3.2. Lateral control

We describe how to control the lateral maneuver of each truck. Consider the case where p_i at time step k heads towards a waypoint whose coordinate is (x_d, y_d). The reference *yaw* angle Ψ^i_k is calculated as

$$\Psi^i_k = \tan^{-1} \frac{y_d - y^i_k}{x_d - x^i_k}. \tag{16}$$

At each time step k, we control the yaw of p_i so that it converges to the reference yaw angle Ψ^i_k. Recall Ψ^i_k is set to make the truck head towards the next waypoint. Let $e_\psi = \Psi^i_k - \psi^i_k$ for convenience.

We change e_ψ so that it exists between $-\pi$ and π. We use

$$e_\psi = \tan^{-1}(\sin(e_\psi)/\cos(e_\psi)). \tag{17}$$

Recall that $\dot{\psi}^i_M = \frac{s^i_k}{T*L^i} \tan(\delta^i_M)$ denotes the maximum yaw rate of a truck p^i. If $\|e_\psi\| > \dot{\psi}^i_M * T$, then we set the steering angle as

$$\delta^i_k = sign(e_\psi) * \delta^i_M. \tag{18}$$

The third equation of (1) is

$$\psi^i_{k+1} = \psi^i_k + T * \frac{s^i_k}{L^i} \tan(\delta^i_k). \tag{19}$$

(18) and (19) lead to

$$\psi^i_{k+1} = \psi^i_k + sign(e_\psi) * \dot{\psi}^i_M * T. \tag{20}$$

Here, $sign(e_\psi)$ denotes the sign of e_ψ. This implies that we change the yaw of the truck with maximum yaw rate $\dot{\psi}^i_M$.

If $\|e_\psi\| \leq \dot{\psi}^i_M * T$, then we set the steering angle as

$$\delta^i_k = \tan^{-1}\left(\frac{e_\psi * L^i}{T * s^i_k}\right). \tag{21}$$

(21) and (19) lead to

$$\psi^i_{k+1} = \Psi^i_k. \tag{22}$$

This implies that the yaw angle of the truck converges to the reference yaw angle.

3.3. Collision avoidance

We need to handle the case where a truck is too close to its predecessor truck. In other words, we handle the case where $D^{i-1,i}_k < safeD$. Recall that the distance between p^i and p^{i-1} at time step k is $D^{i-1,i}_k = \|\mathbf{P}^i_k - \mathbf{P}^{i-1}_k\|$. Also, $safeD > 0$ is the minimum distance between neighboring trucks for safety. If this dangerous case happens, then p^i needs to stop abruptly to avoid collision. Thus, we set the reference speed r^i_k as zero in the case where $D^{i-1,i}_k < safeD$ is satisfied.

 doi:10.20944/preprints202006.0066.v1

Peer-reviewed version available at Appl. Sci. 2020, 10, 5067; doi:10.3390/app10155067

Even in the case where we set the reference speed r_k^i as zero, it takes some time to decrease the truck's speed from s_k^i to zero. The required time to stop is $\frac{s_k^i}{a_D^i}$. Then, the travel distance of the truck while decreasing its speed to zero is $\frac{(s_k^i)^2}{2*a_D^i}$. To avoid collision, it is desirable to set $safeD$ so that

$$safeD > \frac{(s_k^i)^2}{2 * a_D^i} \tag{23}$$

is satisfied. However, as $safeD$ increases, the separation between neighboring trucks increases. Thus, the effect of fuel reduction under truck platoon decreases. Thus, there is a trade-off between fuel reduction and vehicle safety.

3.4. Sensor requirements

(9) implies that a truck p^i needs to access $D_k^{i-1,i}$ and s_k^{i-1}. To enable this, each truck needs to access the position and speed of its predecessor truck. These data are accessible using local sensors, such as radar, lidar, or local communication with its predecessor truck. Moreover, in practice, sensor noise exists in the measurements of $D_k^{i-1,i}$ and s_k^{i-1}. In simulations (Section 4), we added Gaussian noise in the measurements of $D_k^{i-1,i}$ and s_k^{i-1}.

(16) implies that every truck heads towards the next waypoint at each time step. To enable this, each truck localizes itself in the global coordinate system using various sensors, such as Lidar, Distance Measurement Instruments (DMI), Global Positioning Systems (GPS) or Inertial Measurement Units (IMU). [1] Also, using V2V communication [30], the leader's waypoint information is transmitted to every following truck.

4. MATLAB Simulations

We present MATLAB simulations to verify our control laws. The initial speed of every heterogeneous truck is zero. We used (1) to model the motion of every truck.

Our simulation settings are as follows. As a method to simulate localization error in the waypoints, we added a Gaussian noise with mean 0 and standard deviation 0.1 (m) to each element in every waypoint. This error is associated to GPS error which exists in practice.

Recall that a truck p^i needs to access $D_k^{i-1,i}$ and s_k^{i-1} in (9). A truck accesses these values using local sensors, such as radar or lidar, or local communication with p^{i-1}. Considering noise in local measurements, we added a Gaussian noise with mean 0 and standard deviation 0.1 (m) to $D_k^{i-1,i}$. Also, we added a Gaussian noise with mean 0 and standard deviation 0.01 (m/s) to speed measurements in s_k^{i-1}.

In simulations, we use the following variables. $g = 1$, $t_d = 0.01$, $T = 0.5$ (s), $min_D = 1$ (m), $safeD = 0.5$ (m) and $\delta_M^i = 30$ degrees. For all $i \in \{1, 2, ..., N\}$, s_M^i is 80 km/h.

We simulate heterogeneous trucks as follows. In the case where $mod(j, 3)$ is 0, $L^j = 10$ (m). Also, $a_A^j = 1.5m/s^2$ and $a_D^j = 2m/s^2$. In the case where $mod(j, 3)$ is 1, $L^j = 5$ (m). Also, $a_A^j = 1m/s^2$ and $a_D^j = 2m/s^2$. In the case where $mod(j, 3)$ is 2, $L^j = 3$ (m). Also, $a_A^j = 2m/s^2$ and $a_D^j = 2m/s^2$. Using (4), each truck with distinct length has distinct maximum yaw rate. In this way, we consider heterogeneous trucks composed of various kinds of trucks.

In practice, the leader is controlled by a trained truck driver. In simulations, the leader truck follows one lane initially. We also simulate the case where the leader changes its lane to avoid obstacles.

[1] Localization based on multiple sensors is not within the scope of this paper and is presented in various papers, such as [31–33]. In the case where there are sensing or communication infrastructure along a road, we can use the infrastructure to localize a truck. In order to localize a truck, many estimation methods were utilized, such as time of arrival (TOA), time difference of arrival (TDOA), angle of arrival (AOA), and received signal strength [34–45].

Preprints (www.preprints.org) | NOT PEER-REVIEWED | Posted: 7 June 2020 doi:10.20944/preprints202006.0066.v1

Peer-reviewed version available at Appl. Sci. 2020, 10, 5067; doi:10.3390/app10155067

The leader increases its speed with the maximum acceleration a_A^1 until the speed reaches 80 km/h. Then, the leader maintains its speed as 80 km/h using ACC. After the leader moves for 16 minutes, the scenario ends.

Figure 2 (a) shows the lanes that the trucks follow. Also, (b) shows the trajectory of every truck. Initially, five trucks are located at $[0, 3]$,$[-0.001, 3]$, $[-0.002, 3]$,$[-0.003, 3]$,$[-0.004, 3]$ in km.

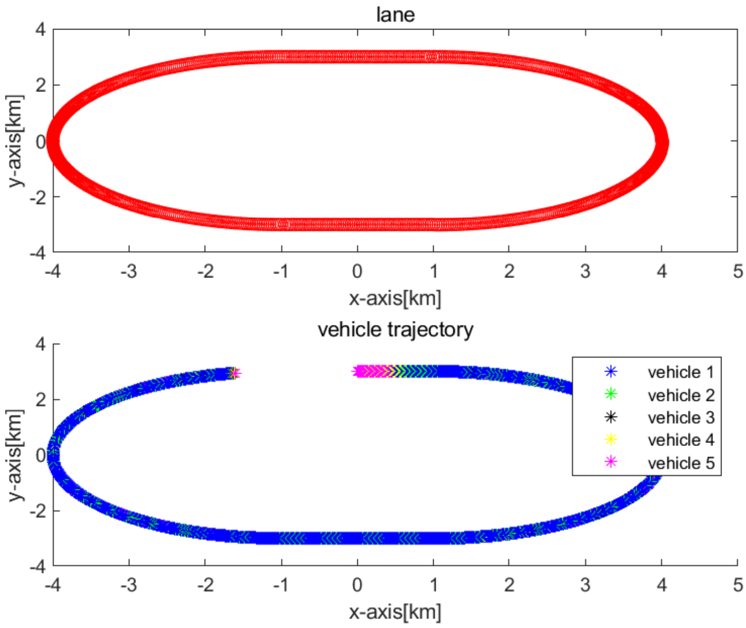

Figure 2. (a) shows the lanes that the trucks follow. Also, (b) shows the trajectory of every truck.

Figure 3 shows the enlarged figure of Figure 2 (a). Waypoints of the leader are shown with red circles. We simulate the case where the leader changes its lane to avoid obstacles. See that waypoints jump from one lane to another. The jump is marked with an arrow in this figure.

Figure 4 shows the speed of each heterogeneous truck with respect to time(sec). We use $\gamma = 1.01$. The speed of every truck converges to the speed of the leader (truck 1) as time goes on. Due to the noise in the system, the truck speed is also noisy.

Figure 5 shows the separation between every neighboring truck. Initially, the separation between neighboring trucks increases. However, the separation converges to the desired separation as time goes on.

4.0.1. The effect of changing γ

Next, we analyze the effect of changing γ. Figure 6 shows the speed of each heterogeneous truck with respect to time(sec). The only difference from Figure 4 is that we use $\gamma = 1.001$ instead of $\gamma = 1.01$. See that the deviation of every truck's speed decreased, compared to the case where $\gamma = 1.01$ in Figure 4. Due to the noise in the system, the truck speed is also noisy.

Figure 7 shows the separation between every neighboring truck. Initially, the separation between neighboring trucks increases. See that it takes more time in making the separation converge to the desired separation, compared to the case where $\gamma = 1.01$ in Figure 5.

4.0.2. The effect of Gaussian noise

Next, we analyze the effect of Gaussian noise. We use $\gamma = 1.01$. No Gaussian noise is added to $D_k^{i-1,i}$. Also, no Gaussian noise is added to speed measurements in s_k^{i-1}.

Figure 8 shows the speed of each heterogeneous truck with respect to time(sec). The only difference from Figure 4 is that no Gaussian noise is used. See that the deviation of every truck's speed

Preprints (www.preprints.org) | NOT PEER-REVIEWED | Posted: 7 June 2020 doi:10.20944/preprints202006.0066.v1
Peer-reviewed version available at Appl. Sci. 2020, 10, 5067; doi:10.3390/app10155067

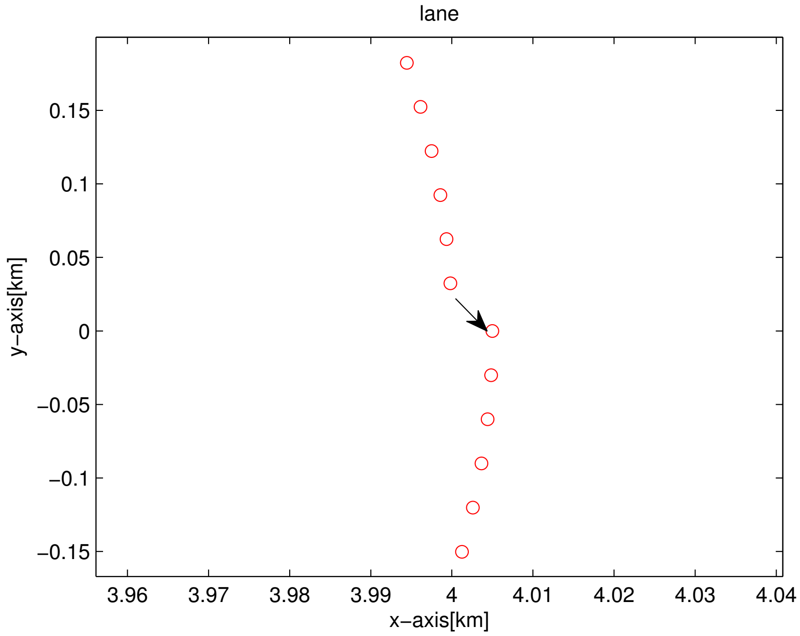

Figure 3. This figure shows the enlarged figure of Figure 2 (a). Waypoints of the leader are shown with red circles. We simulate the case where the leader changes its lane to avoid obstacles. See that waypoints jump from one lane to another. The jump is marked with an arrow in this figure.

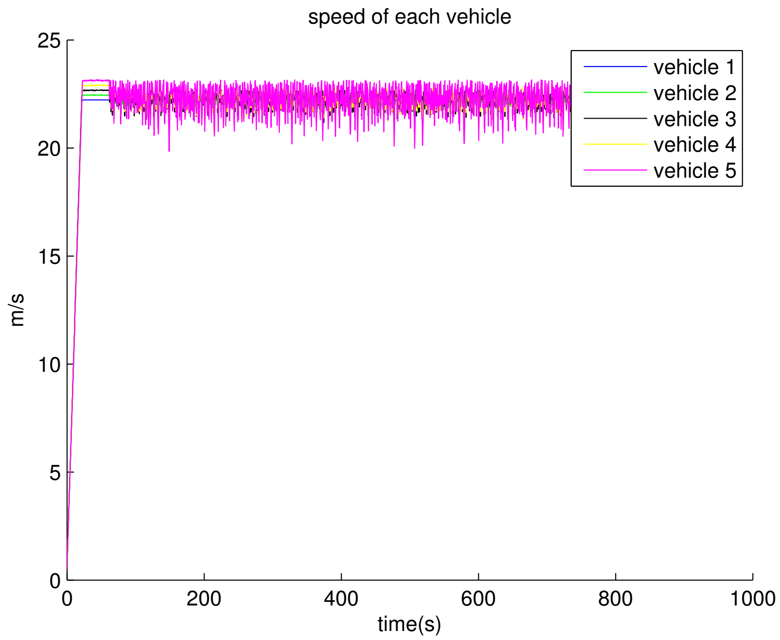

Figure 4. We use $\gamma = 1.01$. The speed of every truck converges to the speed of the leader as time goes on. Due to the noise in the system, the truck speed is also noisy.

Preprints (www.preprints.org) | NOT PEER-REVIEWED | Posted: 7 June 2020 doi:10.20944/preprints202006.0066.v1

Peer-reviewed version available at Appl. Sci. 2020, 10, 5067; doi:10.3390/app10155067

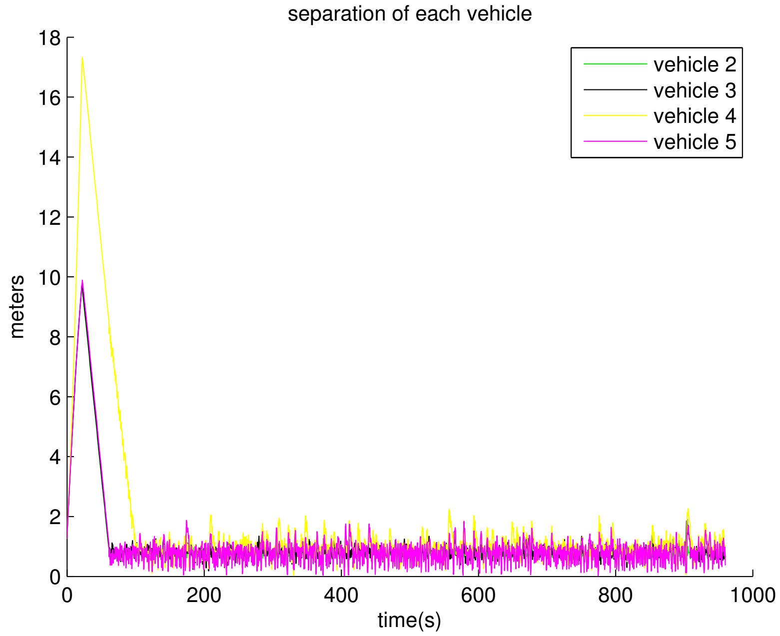

Figure 5. This figure shows the separation between every neighboring truck. We use $\gamma = 1.01$. The separation converges to the desired separation as time goes on.

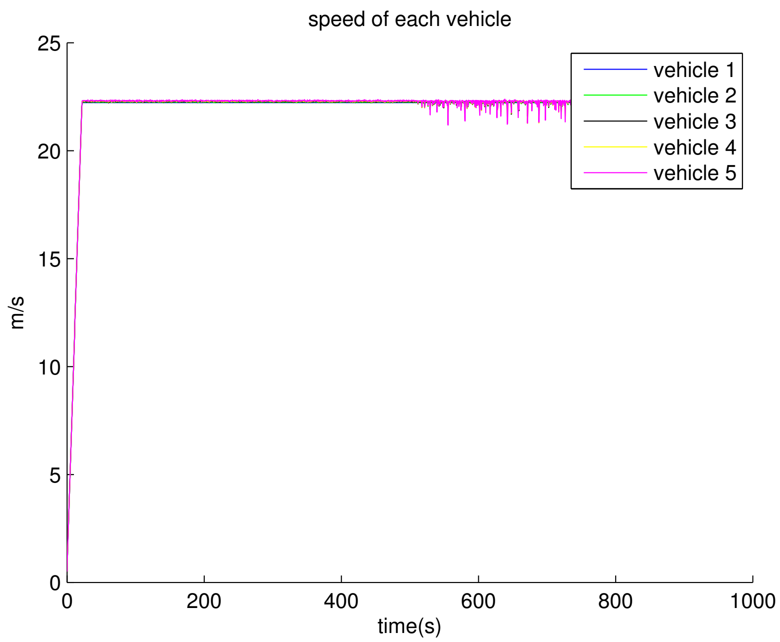

Figure 6. The speed of every heterogeneous truck converges to the speed of the leader as time goes on. We use $\gamma = 1.001$. See that the deviation of every truck's speed decreased, compared to the case where $\gamma = 1.01$ in Figure 4. Due to the noise in the system, the truck speed is also noisy.

Peer-reviewed version available at Appl. Sci. 2020, 10, 5067; doi:10.3390/app10155067

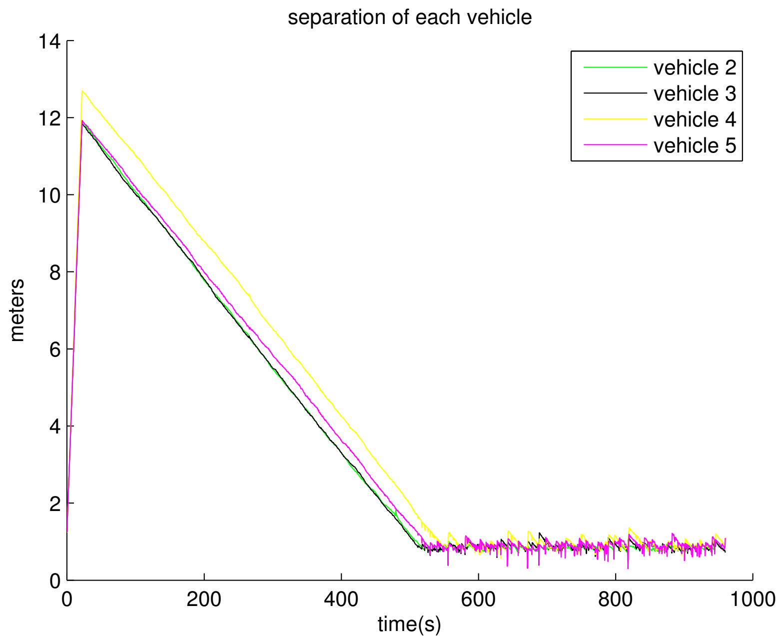

Figure 7. This figure shows the separation between every neighboring truck (scenario 2). We use $\gamma = 1.001$. See that it takes more time in making the separation converge to the desired separation, compared to the case where $\gamma = 1.01$ in Figure 5.

decreased, compared to the case where Gaussian noise is used. A truck speed overshoot (marked with arrow in Figure 8) happens at the moment when the truck changes its lane. See Figure 3 for the moment when the truck changes its lane.

Figure 9 shows the separation between every neighboring truck. The only difference from Figure 5 is that no Gaussian noise is used. Initially, the separation between neighboring trucks increases. See that the deviation of every truck's separation decreased, compared to the case where Gaussian noise is used (Figure 5).

5. Conclusions

This paper presents control algorithms enabling heterogeneous trucks to drive in platoons. We make all heterogeneous trucks keep following waypoints along the leader's trajectory. Every truck visits the leader's waypoints sequentially while maintaining a designated distance from its predecessor truck. As far as we know, this paper is unique in developing both lateral maneuver and speed control considering a platoon of heterogeneous trucks. The efficiency of the proposed approach is verified using simulations. As our future works, we will verify the effectiveness of the proposed approach using experiments with real heterogeneous trucks.

Funding: This work was supported by the National Research Foundation of Korea(NRF) grant funded by the Korea government(MSIT) (No. 2019R1F1A1063151), and 2020 Hongik University Research Fund.

Conflicts of Interest: "The authors declare no conflict of interest."

References

1. Khalifa, A.; Kermorgant, O.; Dominguez, S.; Martinet, P. Vehicles Platooning in Urban Environment: Consensus-based Longitudinal Control with Limited Communications Capabilities. 2018 15th International Conference on Control, Automation, Robotics and Vision (ICARCV), 2018, pp. 809–814. doi:10.1109/ICARCV.2018.8581142.
2. Turri, V.; Besselink, B.; Johansson, K.H. Cooperative Look-Ahead Control for Fuel-Efficient and Safe Heavy-Duty Vehicle Platooning. *IEEE Transactions on Control Systems Technology* **2017**, *25*, 12–28.

Peer-reviewed version available at *Appl. Sci.* **2020**, *10*, 5067; doi:10.3390/app10155067

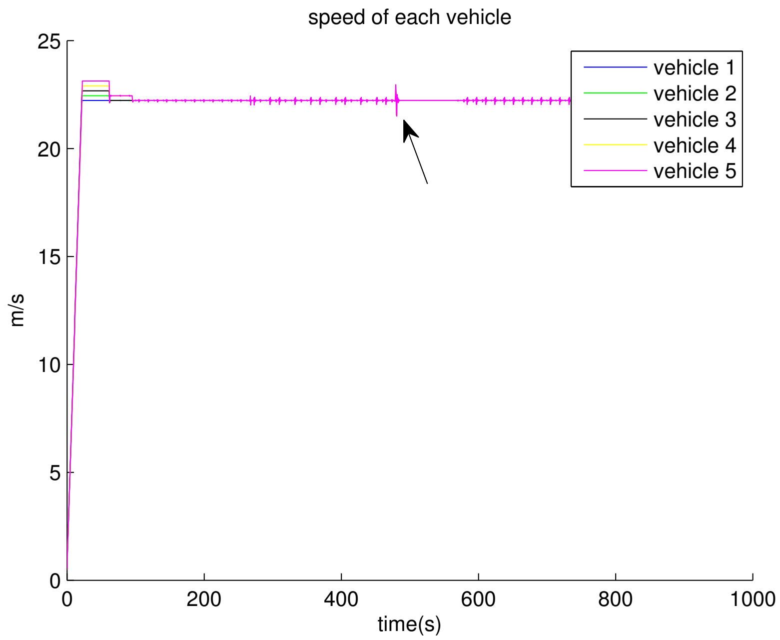

Figure 8. The speed of every heterogeneous truck converges to the speed of the leader as time goes on. We use $\gamma = 1.01$. No Gaussian noise is used. See that the deviation of every truck's speed decreased, compared to the case where Gaussian noise is used. A truck speed overshoot (marked with arrow in Figure 8) happens at the moment when the truck changes its lane. See Figure 3 for the moment when the truck changes its lane.

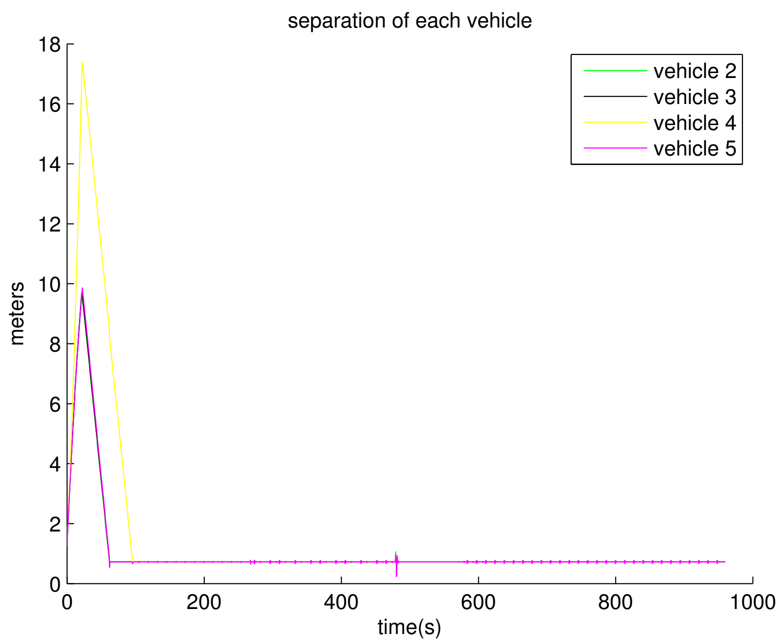

Figure 9. This figure shows the separation between every neighboring truck (scenario 2). We use $\gamma = 1.01$. No Gaussian noise is used. See that the deviation of every truck's separation decreased, compared to the case where Gaussian noise is used (Figure 5).

3. van de Hoef, S.; Johansson, K.H.; Dimarogonas, D.V. Fuel-Efficient En Route Formation of Truck Platoons. *IEEE Transactions on Intelligent Transportation Systems* **2018**, *19*, 102–112.
4. Mechat, N.; Saadia, N.; M'Sirdi, N.; Djelal, N. Lane detection and tracking by monocular vision system in road vehicle. 5th International Congress on Image and Signal Processing; , 2012; pp. 1276 – 1282.
5. Seo, Y.; Rajkumar, R.R. Detection and tracking of boundary of unmarked roads. 17th International Conference on Information Fusion (FUSION); , 2014; pp. 1–6.
6. Jung, C.R.; Kelber, C.R. A robust linear-parabolic model for lane following. Proceedings. 17th Brazilian Symposium on Computer Graphics and Image Processing; , 2004; pp. 72–79.
7. Kim, J.; Zhang, F.; Egerstedt, M. Curve Tracking Control for Autonomous Vehicles with Rigidly Mounted Range Sensors. *Journal of Intelligent and Robotic Systems* **2009**, *56*, 177–197. doi:10.1007/s10846-009-9308-z.
8. Kim, J. Control laws to avoid collision with three dimensional obstacles using sensors. *Ocean Engineering* **2019**, *172*, 342 – 349.
9. Kim, J. Boundary Tracking Control for Autonomous Vehicles with Rigidly Mounted Range Sensors. *Journal of Intelligent & Robotic Systems* **2018**. doi:10.1007/s10846-018-0923-4.
10. Ploeg, J.; van de Wouw, N.; Nijmeijer, H. Lp String Stability of Cascaded Systems: Application to Vehicle Platooning. *IEEE Transactions on Control Systems Technology* **2014**, *22*, 786–793.
11. Martinez, J.; Canudas-de-Wit, C. A Safe Longitudinal Control for Adaptive Cruise Control and Stop-and-Go Scenarios. *IEEE Transactions on Control Systems Technology* **2007**, *15*, 246–258. doi:10.1109/TCST.2006.886432.
12. Xiao, L.; Gao, F. Practical String Stability of Platoon of Adaptive Cruise Control Vehicles. *IEEE Transactions on Intelligent Transportation Systems* **2011**, *12*, 1184–1194. doi:10.1109/TITS.2011.2143407.
13. Ioannou, P.A.; Chien, C.C. Autonomous intelligent cruise control. *IEEE Transactions on Vehicular Technology* **1993**, *42*, 657–672. doi:10.1109/25.260745.
14. Flores, C.; Milanés, V.; Nashashibi, F. A time gap-based spacing policy for full-range car-following. 2017 IEEE 20th International Conference on Intelligent Transportation Systems (ITSC), 2017, pp. 1–6. doi:10.1109/ITSC.2017.8317793.
15. D., S.; K., H.J. Constant Spacing Strategies for Platooning in Automated Highway Systems. *ASME. J. Dyn. Sys., Meas., Control* **1999**, *121(3)*, 462–470.
16. Song, M.; Chen, F.; Ma, X. A Simulation of the Traffic Behavior with Autonomous Truck Platoons Based on Cellular Automaton. 2019 5th International Conference on Transportation Information and Safety (ICTIS), 2019, pp. 416–423. doi:10.1109/ICTIS.2019.8883834.
17. Sadraddini, S.; Sivaranjani, S.; Gupta, V.; Belta, C. Provably Safe Cruise Control of Vehicular Platoons. *IEEE Control Systems Letters* **2017**, *1*, 262–267.
18. Molnar, T.G.; Qin, W.B.; Insperger, T.; Orosz, G. Application of Predictor Feedback to Compensate Time Delays in Connected Cruise Control. *IEEE Transactions on Intelligent Transportation Systems* **2018**, *19*, 545–559.
19. VanderWerf, J.; Shladover, S.; Kourjanskaia, N.; Miller, M.; Krishnan, H. Modeling Effects of Driver Control Assistance Systems on Traffic. *Transportation Research Record* **2001**, *1748*, 167–174, [https://doi.org/10.3141/1748-21]. doi:10.3141/1748-21.
20. Chehardoli, H.; Ghasemi, A. Formation control of longitudinal vehicular platoons under generic network topology with heterogeneous time delays. *Journal of Vibration and Control* **2019**, *25*, 655–665.
21. Xiao, L.; Gao, F. Practical String Stability of Platoon of Adaptive Cruise Control Vehicles. *IEEE Transactions on Intelligent Transportation Systems* **2011**, *12*, 1184–1194.
22. Saeednia, M.; Menendez, M. A Consensus-Based Algorithm for Truck Platooning. *IEEE Transactions on Intelligent Transportation Systems* **2017**, *18*, 404–415.
23. Li, M.; Chen, Y.; Zhou, A.; He, W.; Li, X. Adaptive tracking control for networked control systems of intelligent vehicle. *Information Sciences* **2019**, *503*, 493 – 507.
24. Guo, G.; Wang, Q. Fuel-Efficient En Route Speed Planning and Tracking Control of Truck Platoons. *IEEE Transactions on Intelligent Transportation Systems* **2019**, *20*, 3091–3103. doi:10.1109/TITS.2018.2872607.
25. Chehardoli, H.; Ghasemi, A. Adaptive Centralized/Decentralized Control and Identification of 1-D Heterogeneous Vehicular Platoons Based on Constant Time Headway Policy. *IEEE Transactions on Intelligent Transportation Systems* **2018**, *19*, 3376–3386.
26. LaValle, S.M. *Planning Algorithms*; Cambridge, 2006.

27. Berntorp, K.; Olofsson, B., L.; K..; Nielsen, L. Models and methodology for optimal trajectory generation in safety-critical road-vehicle manoeuvres. *Vehicle System Dynamics* **2014**, *52(10)*, 1304–1332.
28. Kim, J. Analysis of handling performance based on simplified lateral vehicle dynamics. *International Journal of Automotive Technology* **2008**, *9(6)*, 687–693.
29. Mashadi, B.; Mahmoudi-Kaleybar, M.; Ahmadizadeh, P.; Oveisi, A. A path-following driver/vehicle model with optimized lateral dynamic controller. *Latin American Journal of Solids and Structures* **2014**, *11*, 613 – 630.
30. Bergenhem, C.; Hedin, E.; Skarin, D. Vehicle-to-Vehicle Communication for a Platooning System. *Procedia - Social and Behavioral Sciences* **2012**, *48*, 1222–1233.
31. X, M.; H, W.; B., L. A Robust Vehicle Localization Approach Based on GNSS/IMU/DMI/LiDAR Sensor Fusion for Autonomous Vehicles. *Sensors (Basel)* **2017**, *17(9)*, 1–19.
32. Chen, L.; Hu, H. IMU/GPS based pedestrian localization. 2012 4th Computer Science and Electronic Engineering Conference (CEEC), 2012, pp. 23–28.
33. Saadeddin, K.; Abdel-Hafez, M.F.; Jarrah, M.A. Estimating Vehicle State by GPS/IMU Fusion with Vehicle Dynamics. *Journal of Intelligent Robotic Systems* **2014**, *74(1-2)*, 147–172.
34. Kim, J. Fast non-line-of-sight receivers conjecturing method in TDOA localisation using obstacle information. *IET Radar, Sonar and Navigation* **2019**, *13*, 347–351(4).
35. Howard, A.; Mataric, M.; Sukhatme, G. Relaxation on a mesh: a formalism for generalized localization. Proc. of IEEE/RSJ International Conference on Intelligent Robots and Systems; , 2001; pp. 1055 – 1060.
36. Mao, G.; Fidan, B.; Anderson, B.D. Wireless sensor network localization techniques. *Computer Networks* **2007**, *51*, 2529 – 2553.
37. Priyantha, N.B.; Balakrishnan, H.; Demaine, E.; Teller, S. anchor-free distributed localization in sensor networks. Proc. of the first international conference on Embedded networked sensor system; , 2001; pp. 340 – 341.
38. Jiang, J.R.; Lin, C.M.; Lin, F.Y.; Huang, S.T. ALRD: AoA Localization with RSSI Differences of Directional Antennas for Wireless Sensor Networks. *International Journal of Distributed Sensor Networks* **2013**, *2013*, Article ID 529489.
39. Han, G.; Xu, H.; Duong, T.Q.; Jiang, J.; Hara, T. Localization algorithms of Wireless Sensor Networks: a survey. *Telecommunication Systems* **2013**, *52*, 2419–2436.
40. Cheng, L.; Wu, C.; Zhang, Y.; Wu, H.; Li, M.; Maple, C. A Survey of Localization in Wireless Sensor Network. *International Journal of Distributed Sensor Networks* **2012**, *2012*, Article ID 962523.
41. Niculescu, D.; Nath, B. Ad hoc positioning system (APS) using AOA. Twenty-Second Annual Joint Conference of the IEEE Computer and Communications; , 2003; pp. 1734 – 1743.
42. Assaad, A.E.; Krug, M.; Fischer, G. Vehicle self-localization for advanced driver assistance systems. 13th Workshop on Positioning, Navigation and Communications (WPNC); , 2016; pp. 1 – 6.
43. Fascista, A.; Ciccarese, G.; Coluccia, A.; Ricci, G. Angle of Arrival- Based Cooperative Positioning for Smart Vehicles. *IEEE Transactions on Intelligent Transportation Systems* **2017**, *PP*, 1 – 13.
44. Alam, N.; Balaei, A.T.; Dempster, A.G. An Instantaneous Lane-Level Positioning Using DSRC Carrier Frequency Offset. *IEEE Transactions on Intelligent Transportation Systems* **2012**, *13*, 1566 – 1575.
45. Gustafsson, F. *Statistical Sensor Fusion*; Studentlitteratur: Sweden, 2012.